Rheological Behavior of Entangled Polystyrene−Polyhedral Oligosilsesquioxane (POSS) Copolymers

Jian Wu,[†,⊥] Timothy S. Haddad,[‡] Gyeong-Man Kim,[§] and Patrick T. Mather*[,†,∥]

Polymer Program and Department of Chemical Engineering, University of Connecticut, Storrs, Connecticut 06269, ERC, Inc., AFRL/PRSM, Edwards Air Force Base, California 93524, Institut für Werkstoffwissenschaft, Martin-Luther-Universität Halle-Wittenberg, Geusaer Strasse, D-06217 Merseburg, Germany

Received August 15, 2006; Revised Manuscript Received November 11, 2006

ABSTRACT: We report on the linear viscoelastic properties of a family of entangled linear thermoplastic nonpolar hybrid inorganic−organic polymers: random copolymers of polystyrene (PS) and styryl-based polyhedral oligosilsesquioxane (POSS), $R_7(Si_8O_{12})(C_6H_4CH{=}CH_2)$, with R = isobutyl (^{i}Bu). A series of styrene−styryl POSS random copolymers with 0, 6, 15, 30, and 50 wt % ^{i}BuPOSS were investigated. WAXS and TEM demonstrate that the ^{i}BuPOSS disperses in the polymeric matrix at a molecular level. It is observed that the ^{i}BuPOSS plays a plasticizer-like effect, yielding a monotonic decrease of the glass-transition temperature with increasing ^{i}BuPOSS content. Rheological measurements revealed that linear viscoelastic behavior of the copolymers is also profoundly influenced by the presence of ^{i}BuPOSS. The incorporation of ^{i}BuPOSS dramatically decreases the rubbery plateau modulus (G_N^o), suggesting a strong dilation effect of isobutyl−POSS on entanglement density. Additionally, the apparent flow activation energy, obtained by fitting the Vogel−Fulcher−Tamman−Hesse equation, monotonically increases with increasing ^{i}BuPOSS content, indicating a lower sensitivity of POSS copolymers to changes of temperature. We attribute our observations to the microscopic topology of constituent polymer chains to be altered by ^{i}BuPOSS comonomers that act as compact volumetric branches. Conversely, intermolecular interactions between ^{i}BuPOSS and PS segments do not play an essential role in determining the rheological behavior.

1. Introduction

As an alternative to conventional polymer−matrix composites, materials engineers have begun turning to approaches that improve properties by reinforcing the constituent polymer chains at the local, or segmental, level. One particularly successful approach has been the use of hybrid inorganic−organic monomeric units, polyhedral oligosilsesquioxane (POSS), that feature aspects of organic functionality required for intimate dispersion and mechanically rigid silicon−oxygen polyhedral reinforcement, allowing molecular reinforcement. POSS monomers are functionalized with not only a polymerizable group or groups but also with inert organic groups at the other vertices and are within the nanomaterials classification. The size of POSS, consisting of an inorganic (silicon−oxygen) core and eight variable organic side groups, is approximately 1.5 nm. Moreover, POSS aggregation to large (∼50 nm) but limited scale is commonly observed. The present work addresses the importance of aggregation (or lack thereof) in determining physical properties.

The introduction of POSS moieties pendent to the polymeric chain has a dramatic effect on the physical properties of the polymeric materials, which was detailed in a comprehensive review paper by Li and co-workers.[1] For polystyrene,[2] polynorbornene,[3] and poly(methyl methacrylate)[4] tethered by cyclopentyl−POSS (CpPOSS) and cyclohexyl−POSS (CyPOSS), the T_g monotonically increases with POSS incorporation. The retardation of polymer chain motion has been thought to be ascribed to the interaction or association between POSS groups, and/or a large inertia effect on the segmental mobility due to the massive POSS groups.[5] This observation is also true for thermosetting networks. For a POSS−epoxy system, Lee and Lichtenhan revealed a retardation effect that hinders the molecular motion of an epoxy network junction.[6] Surprisingly, their small-strain stress relaxation experiments revealed that monofunctional POSS moieties had no contribution to the deformation process of the epoxy network, and it was concluded that multifunctionality would be required for such an effect. Meanwhile, Li et al. extensively studied the influence of multifunctional POSS on viscoelastic properties of copolymers, revealing the significant role played by POSS incorporation.[7,8] However, only a few reports on the rheological behavior pertaining to the linear polymers tethered by POSS exist. Romo-Uribe et al.[9] reported the linear viscoelastic properties of unentangled random copolymers from 4-methylstyrene and its POSS derivatives with R = cyclopentyl (Cp) and cyclohexyl (Cy). There, the rheological properties were profoundly altered with increasing POSS incorporation. At higher mole fractions of POSS (CpPOSS > 16 mol % and CyPOSS > 8 mol %), a secondary rubbery plateau with $G' \sim 10^3$ Pa appeared, replacing the expected traditional terminal zone behavior of unfunctionalized poly(4-methylstyrene). This phenomenon was attributed to intermolecular interactions involving two POSS moieties.

More generally, for polymeric liquids that feature specific interchain interactions, an additional relaxation time may appear in the rheological spectrum, either shorter than or longer than the unmodified terminal (longest) relaxation time. Moreover,

* Corresponding author. E-mail: patrick.mather@case.edu.
† Polymer Program and Department of Chemical Engineering, University of Connecticut.
‡ ERC, Inc., AFRL/PRSM, Edwards Air Force Base.
§ Institut für Werkstoffwissenschaft, Martin-Luther-Universität Halle-Wittenberg.
∥ Present address: Macromolecular Science and Engineering, Case Western Reserve University, 2100 Adelbert Rd., Cleveland, Ohio 44106.
⊥ Present address: Chemical Engineering Department, Texas Tech University, Lubbock, Texas 79410.

10.1021/ma061886f CCC: $37.00
Published on Web 01/09/2007

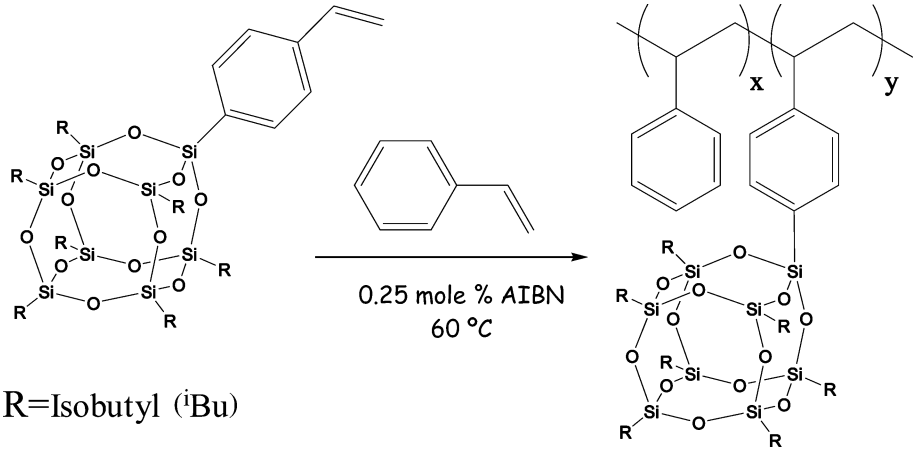

Figure 1. Synthetic scheme for the preparation of random copolymers yielded from styrene− and styryl−isobutylPOSS(iBuPOSS) through radical copolymerization initiated by AIBN at 60 °C.

such association sites can act the way entanglements do, leading to a decrease of the entanglement molecular weight in an already entangled polymeric liquid as well as a secondary rubbery plateau if the associated relaxation times are sufficiently separated. This mechanism can be described by the "sticky reptation" model developed by Leibler et al.[10] and conceived for the hydrogen-bonded elastomers.[11,12] Indeed, more recent activity in the field of supramolecular polymers has witnessed similar phenomena.[13,14] Unfortunately, because of the limited polymerization degree, observations of this type for POSS's impact on the rubbery plateau were impossible for the system previously studied. However, recent reports from Kopesky et al.[15, 16] found that tethered-POSS incorporated within entangled poly(methyl methacrylate) (PMMA)-based copolymers featured decreasing plateau modulus (G_N^o) relative to PMMA homopolymer, motivating the present work.

How might POSS impact the state of entanglement for a polymer melt? Answering this question is the primary objective of the present work. Architecturally, POSS moieties pendent to a polymeric backbone are similar to the random branches with spherical shape that are intrinsically incapable of entangling with each other or the backbone chains. Recognizing that chain topology of entangled linear polymeric liquids impacts viscoelastic behavior as explained with the reptation (or tube) model,[17] the rubbery plateau modulus, G_N^o, depends on contour properties characterized by contour length L_{pp}, tube diameter d_T, Kuhn length a_{PP}, and packing length l_p that we hypothesize to be influenced by the pendent POSS moieties. Fetters et al.[18] introduced the empirical universal relation for G_N^o (Pa) and l_p (Å):

$$G_N^o = 0.00226 k_B T / l_p^3 \qquad (1)$$

where k_B and T are Boltzmman constant (1.38×10^{-23} m^2·kg/s^2·K) and absolute temperature (K), respectively. This also leads to simple proportionality between tube diameter and packing length: $d_T = 19 l_p$. Recently, Everaer et al.[19] made parameter-free and quantitative predictions for G_N^o through the tube model on the basis of purely topological analysis.

In the present study, we report on the thermal and rheological characterization of entangled random copolymers from styrene and its POSS derivatives with R = isobutyl (iBu) and with systematic variation of the weight percentage of iBuPOSS in the polymers from 0 to 50 wt %. iBuPOSS was selected for this study based on a lack of POSS−POSS aggregation in the PS system, allowing discernment of entangled melt dynamics without complications of physical crosslinking. We observe a profound impact of iBuPOSS incorporation on the glass-transition temperature, the WLF free-volume parameters, and the plateau modulus, all of which are detailed quantitatively. The substantial modification role of pendent POSS group on the rheological properties of polystyrene (PS) will be emphasized. A subsequent report is planned to reveal the impact of POSS R-group variation on rheological properties.

2. Experimental Section

2.1. Synthesis of Styrene-*r*-styryl Isobutyl−POSS (iBuPOSS) Copolymers. Five polymers containing either 0, 6, 15, 30, or 50 wt % POSS−styrene monomer were all synthesized in the same manner as shown in Figure 1. A 10 molal monomer solution containing a total of 3 g of monomers was initiated using 0.25 mol % azobis(isobutyronitrile) (AIBN). One example synthesis of 6 wt % POSS follows: Under a nitrogen atmosphere, a dry O_2-free solution of toluene (2.73 mL), $[(C_8H_7)(i\text{-}C_4H_9)_7(Si_8O_{12})]$ (180 mg, 0.196 mmol), styrene (2820 mg, 27.08 mmol), and AIBN (11.2 mg, 0.068 mmol) was heated to 60 °C for 2 days. This was then diluted with 15 mL of $CHCl_3$ and precipitated into 100 mL of methanol. After stirring 1 h, the copolymer was isolated on fritted glassware and air-dried overnight. ^{1}H NMR spectroscopy (400 MHz) showed no unreacted monomers and confirmed that the product contained 6 wt % POSS.[20] The isolated yield of dry copolymer was 93% of the theoretical value.

The random copolymers prepared from styrene and iBuPOSS−styryl through radical copolymerization were completely dissolved in tetrahydrofuran (THF). The polymer solutions with 5 wt % concentration were poured into Teflon casting dishes to dry at room temperature for 4 days. Next, the cast films were dried under vacuum at 50−60 °C for 2 days and then 80−90 °C for 2 days. In order to remove residual solvent (THF), the cast films were further dried above the glass transition (∼120 °C) for another 12 h. The cast films dried in this manner were employed for further microstructural and physical characterizations.

2.2. Characterization. *2.2.1. Thermal Analysis*. The thermal properties of the random copolymers were investigated by a TA Instruments differential scanning calorimeter (DSC 2920) equipped with a mechanical intercooler (temperature to $T = -60$ °C) under a continuous nitrogen purge (50 mL/min). Both calibrations of heat flow and temperature were based on a run in which one standard sample (indium) was heated through its melting point. The samples from solvent-cast films were sealed in aluminum pans with mass in the range of 5−10 mg. All measurements were conducted at a scan rate of 10 °C/min following a heat−cool−heat procedure from 0 to 250 °C. Glass-transition temperatures (T_g) were determined by the midpoint of a stepwise enthalpy increase during the second heating.

2.2.2. Wide-Angle X-ray Scattering (WAXS). In order to assess the microstructure of the random copolymers, Wide-angle X-ray

Table 1. Summary of Molecular Characteristics of Polystyrene−POSS Copolymers[a,b]

compound	$M_w \cdot 10^3$ (g/mol)	M_w/M_n	DP	wt % POSS	mol % POSS
0 wt % ^{i}BuPOSS	161	1.43	1080	0	0
6 wt % ^{i}BuPOSS	186	1.46	1164	5.9	0.70
15 wt % ^{i}BuPOSS	195	1.40	1158	15.4	2.02
30 wt % ^{i}BuPOSS	300	1.52	1387	33.2	5.34
50 wt % ^{i}BuPOSS	419	1.65	1358	52.1	10.95

[a] Molecular weight and molecular weight distribution were determined by gel permeation chromatography (GPC) in $CHCl_3$, calibrated by polystyrene(PS) standards. [b] DP's are calculated from M_n, and wt % POSS is derived from mol % POSS, which is directly measured from ^{1}H NMR spectroscopy.[20]

scattering (WAXS) experiments were performed at room temperature on the solvent-cast films (as described above) using a BRUKER D5005 X-ray diffractometer with rotating anode source operated at 40 kV and 40 mA. The scattering angle, 2θ, was scanned from 5.0° to 40.0°. Nickel-filtered Cu K_α radiation with wavelength $\lambda = 1.5418$ Å was used for the measurements.

2.2.3. Transmission Electron Microscopy (TEM). Real-space observations of the microstructures adopted by the POSS−PS copolymers were conducted by employing transmission electron microscopy (TEM, JEOL 2010) with an accelerating voltage of 200 kV. The point and line resolution were 0.19 and 0.14 nm, respectively. Thin sections of 50−60 nm thickness were cut at −100 °C using a Leica Ultracut-E microtome equipped with a diamond knife. The thin slices collected on 300 mesh copper TEM grids were stained under RuO_4 vapor at room temperature. Previous work revealed that this staining agent is POSS-selective.[21]

2.2.4. Rheological Characterization. The investigation of linear viscoelastic properties of the random copolymers was conducted by using the ARES rheometer (TA Instruments). It was equipped with two torque transducers distinguished by their torque capacity: 200 g·cm and 2000 g·cm. The existence and extent of the linear viscoelastic regime were determined by the dynamic storage and loss moduli, $G'(\omega)$ and $G''(\omega)$, as a function of strain (0.1−10%) at an angular frequency of 10 rad/s. All of the measurements were carried out within the linear viscoelastic range, where $G'(\omega)$ and $G''(\omega)$ are independent of strain. The dynamic moduli were measured as a function of frequency, ω, spanning 0.01−100 rad/s at temperatures from 120 to 180 °C. All of the rheological characterizations were performed under a nitrogen atmosphere using parallel plates with 8 mm diameter and with the gap between two plates being controlled precisely with a typical value of 1.0 mm.

3. Results and Discussion

3.1. Copolymer Synthesis. Free radical polymerization of the PS−^{i}BuPOSS copolymers led to polymers with high molecular weight (>150 kg/mol) and correspondingly high number-average degrees of polymerization (DP > 1000). Polydispersity indices typical of free radical polymerizations (>1.4) were achieved. In our earlier work, lower monomer concentrations were employed (4 versus 10 molal) and, consequently, significant lower molecular weights were achieved. Table 1 summarizes the molecular characteristics of the copolymers.

3.2. Morphological Characterization. Figure 2 shows the wide-angle X-ray scatting (WAXS) patterns of random copolymers with respect to different content of styryl−isobutylPOSS (^{i}BuPOSS). The WAXS pattern of pure PS shows two amorphous halos: one is centered at a *d*-spacing of 4.5 Å and the other one is at 8.3 Å. These two halos are associated with correlations between main chains ($d = 8.3$ Å) and between phenyl rings ($d = 4.5$ Å), respectively.[22,23] In contrast, the pure styryl−isobutylPOSS macromer is a very crystalline substance and features numerous diffraction peaks. In particular, there is a very intense and sharp diffraction peak at 11.0 Å associated

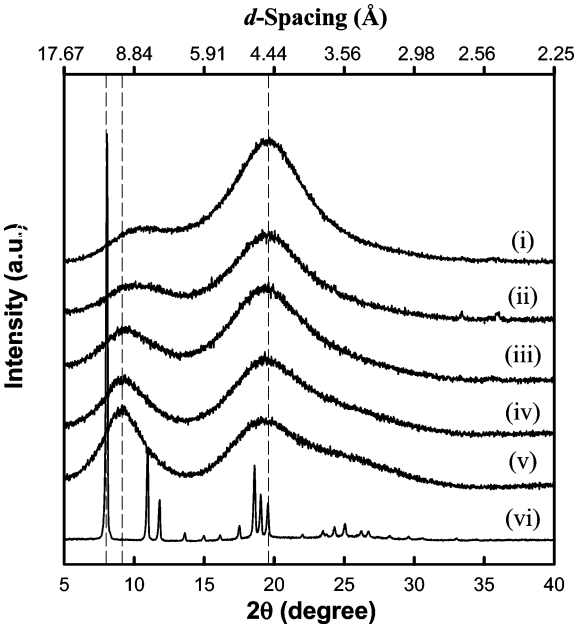

Figure 2. WAXS patterns of as-cast films of ^{i}BuPOSS−PS copolymers with varying weight percentage of ^{i}BuPOSS: (i) 0, (ii) 6, (iii) 15, (iv) 30, (v) 50 wt % ^{i}BuPOSS, and (vi) styryl ^{i}BuPOSS macromer.

with the 101 *hkl* reflection of a rhombohedral lattice.[24] By contrast, no such diffraction peak ascribed to the crystal of ^{i}BuPOSS macromer appears in the WAXS patterns observed for the copolymers. Copolymerization apparently prevents the crystallization of POSS moieties and leads to a good dispersion with a lack of macroscopic ^{i}BuPOSS incorporation. With increasing ^{i}BuPOSS loading, the amorphous halo at the *d*-spacing = 8.3 Å shifts to a lower angle and the corresponding peak is slightly narrowed, indicating that the introduction of ^{i}BuPOSS expands intermolecular main-chain spacing. Meanwhile, the amorphous halo at the *d*-spacing = 4.5 Å slightly broadens, with scattering from the 50 wt % ^{i}BuPOSS sample, revealing the origin to be an emergence of an underlying shoulder peak, which reflects the correlation between ^{i}BuPOSS groups. Furthermore, in contrast with the ^{i}BuPOSS macromer, these two peaks are quite distinct from any crystalline reflections of the ^{i}BuPOSS macromer. The strongest ^{i}BuPOSS reflection peaks appear at *d*-spacings of 11.0 and 8.1 Å; however, these regions of the copolymer WAXD patterns are devoid of any features. Thus it clearly indicates that copolymerization effectively prevents crystallization of ^{i}BuPOSS units.

To further elucidate the microstructure of the random copolymers, we made direct observations of selected samples that were microtomed and selectively stained using transmission electron microscopy (TEM). The dark particles revealed in Figure 3a directly image the POSS-related particles in the sample with 6 wt % ^{i}BuPOSS. The size is only from 1.5 to 3 nm, approaching the size of a single POSS molecule. Further increase in ^{i}BuPOSS concentration leads to the increase of dispersed particle density shown in Figure 3b; however, the particle size nearly does not change. We infer that POSS cages pendent along the PS chain are well-dispersed in the matrix at a molecular level and there is no obvious aggregation of POSS cages, consistent with our WAXS observations described above. The peaks related to the presence of POSS only shift from *d*-spacing centered at 8.3−9.7 Å, implying that the POSS cages are incorporated within the PS chain packing. We conclude that the ^{i}BuPOSS groups grafted on the PS chain were dispersed in the polystyrene matrix at nearly molecular level.

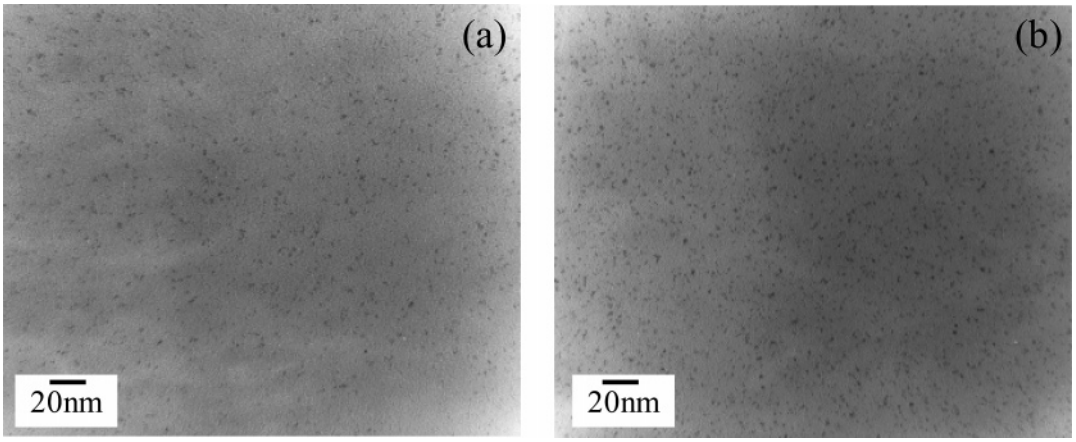

Figure 3. Transmission electron microscopy (TEM) images of as-cast films of ^{i}BuPOSS−PS copolymers: (a) 6, (b) 30 wt % ^{i}BuPOSS. The samples were stained by RuO_4 vapor at ambient condition.

In contrast, we have noticed that POSS aggregation is a commonly observed phenomenon in polynorborene,[3] polyurethane,[25] and polyimide,[26] among others, tethered by POSS molecules. Zheng et al.[27] found that tethered POSS in random copolymers of POSS−polybutadienes can aggregate and closely pack into a two-dimensional lattice. Furthermore, the POSS moiety can aggregate to domains with a size of about 50−60 nm inside a polyimide semi-interpenetrating polymer network (semi-IPN).[28] Additionally, Romo-Uribe et al.[9] reported the both cyclopentyl−POSS (CpPOSS) and cyclohexyl−POSS (CyPOSS) pendent on the poly(4-methylstyrene) can aggregate to form nanocrystals when the POSS loading is increased to a critical mol % content. Zhang et al.[29] studied the effect of random copolymers of PMMA−POSS on the phase segregation of the typical immiscible polymer blend of PMMA and PS prepared from spin-coating. They found that the cyclopentyl-functionalized POSS grafted onto the backbone of PMMA plays a compatibilizing role in a polymer blend of PMMA and PS. It was concluded that a favorable interaction exists between the POSS functional group and the PS homopolymer. So, POSS aggregation essentially depends on the compatibility between POSS molecules and polymer main-chain segments, and there may be a critical concentration beyond which POSS will tend to microphase separate from the matrix. Although the POSS used here is functionalized with isobutyl groups, it is still reasonable for us to expect that ^{i}BuPOSS has the potential to be compatible with PS homopolymer. Indeed, our morphological characterizations have revealed that ^{i}BuPOSS were dispersed with a molecular level, indicating favorable ^{i}BuPOSS−PS interactions.

3.3. Thermal Analysis. The effects of the presence of tethered POSS cages on the glass transition were studied using differential scanning calorimetry (DSC). Second heating traces for the styrene and styryl−^{i}BuPOSS random copolymers are shown in Figure 4. The glass-transition temperatures determined from the midpoint of an enthalpy step increase are shown in Figure 5, where we can observe that the glass-transition temperature of the random copolymers with ^{i}BuPOSS decreases with the increasing POSS content. In addition, we observe a significant and monotonic decrease in the heat capacity change at T_g with increasing POSS loading.

The glass-transition values of polymers reflect, in part, the rotational energy barrier about σ bonds in the backbone chain, lower glass-transition temperatures indicating a lower energy barrier. For polymer families with the same backbone structure, the side chain or group and intermolecular interactions greatly influence T_g. While rigid side chains restrict torsion about σ bonds in the backbone chain, raising T_g, flexible side chains, such as the family of poly(alkyl methacrylate)s,[30] exhibit lowering of T_g by "internal plasticization", where the side group increases interchain spacing and free volume, lowering rotation energy barrier and decreasing T_g. Thus, considering backbone rotation alone, side chains may either increase or decrease T_g, depending on which of the two mentioned factors dominates.

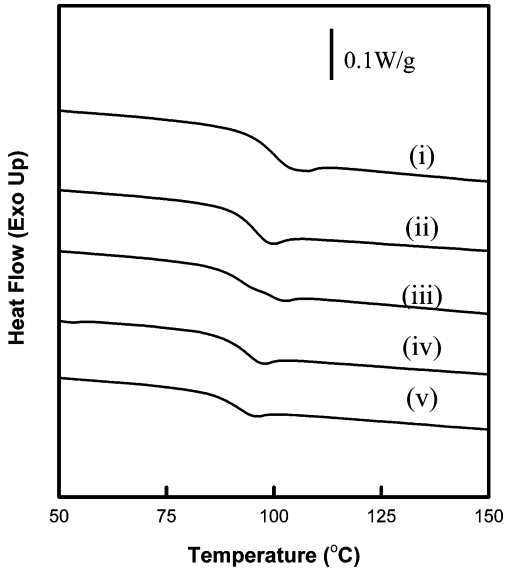

Figure 4. Differential scanning calorimetry (DSC) analysis of as-cast ^{i}BuPOSS−PS copolymers films with varying weight percentage of ^{i}BuPOSS: (i) 0, (ii) 6, (iii) 15, (iv) 30, and (v) 50 wt % ^{i}BuPOSS. The heating rate was 10 °C/min, and the second heating traces are shown.

Additionally, if there is strong intermolecular interaction, such as hydrogen bonding, ion−ion interaction, and acid−base interaction, among others, the formation of physical cross-linking would restrict polymer chain motion, thus enhancing T_g. In POSS-branched polymers, intermolecular interactions consist of both POSS−POSS and POSS−polymer matrixes. The styryl−POSS macromer is functionalized with a polymerizable styrenic group and also decorated with seven inert organic groups (so-called POSS R-group) at other vertices, themselves contributing 80% of the POSS volume and strong R-group sensitivity. For example, POSS incorporation with cyclopentyl(Cp) and cyclohexyl(Cy) R-groups has been uniformly observed to enhance T_g of random copolymers, such as poly(4-methylstyrene−POSS),[2,31] poly(norbornyl−POSS),[3] poly(methacrylate−POSS),[4] and poly(siloxane−POSS),[32] among

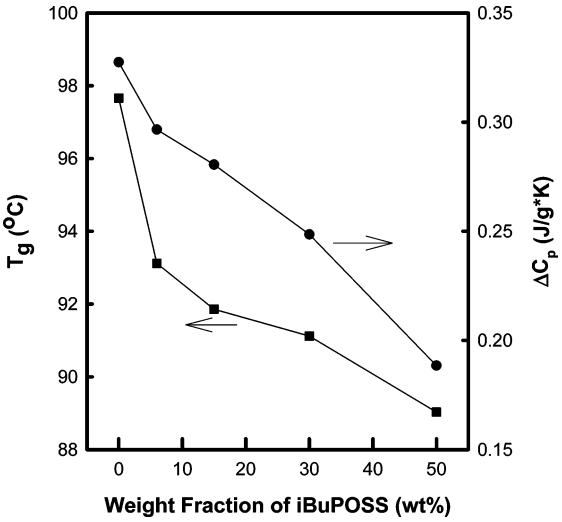

Figure 5. Variation of glass-transition temperature (■, T_g) and heat capacity step change (●, ΔC_p) at T_g as functions of ^{i}BuPOSS content. T_g is determined from the midpoint of enthalpy change in the DSC trace curves shown in Figure 4.

others. However, Xu et al.[33,34] reported that styryl−isobutyl−POSS incorporation into poly(acetoxystyrene)(PAS) and poly(vinylpyrrolidone)(PVP)first *decreases* and then *increases* T_g as the POSS comonomer content is increased.

Here, our copolymers have a polystyrene backbone randomly "branched" by ^{i}BuPOSS. The ^{i}BuPOSS branches effectively increase the distance between adjacent backbone chains, as shown in Figure 2, and lead to the increase of the mean size of local free volume. As a result, the chain mobility is increased and ^{i}BuPOSS, from this factor alone, may play a plasticizing role. However, the massive volume of the POSS cage can undoubtedly induce a steric barrier, increasing the resistance to torsional rotation about σ bonds in the polystyrene backbone chain. Morphological characterization reveals that ^{i}BuPOSS disperse in the PS matrix with a molecular level. Thus, in our samples, the interchain interactions are between molecularly dispersed ^{i}BuPOSS segments and PS segments through relatively weak van der Waals forces. The variation of glass-transition temperature in the random copolymers is the net result of all three effects: free volume, steric barrier, and POSS−polymeric segment interaction. Our DSC data (Figures 4, 5) reveal that the glass transition monotonically decreases, though with upward curvature, with increasing ^{i}BuPOSS content, indicating that the dominant factor in determining T_g is the addition of free volume effect by ^{i}BuPOSS. This interpretation will be further supported with rheological measurements employing time−temperature superposition.

3.4. Rheological Behavior. *3.4.1. Time Temperature Superposition.* We investigated the applicability of time−temperature superposition (TTS) to the subject PS−POSS copolymers by conducting frequency sweep tests spanning the temperature range 120 °C < T < 180 °C. This limited range was selected in order to avoid thermal degradation and side reactions, yet feature enough sample compliance to avoid exceeding the torque limit of the instrument. All of the experiments were within the linear viscoelastic regime determined by strain sweep tests. Relative to a fixed reference temperature (T = 120 °C), we established the time−temperature superposition (TTS) by shifting the logarithmic plots of $G'(\omega)$ and $G''(\omega)$ along the frequency axis (horizontally). Vertical shifts along the modulus axis were not required. Thus, for good superposition,

$$G'(\omega,T) = G'(a_T\omega,T_r) \tag{2}$$

$$G''(\omega,T) = G''(a_T\omega,T_r) \tag{3}$$

where T_r is the reference temperature and a_T are the temperature-dependent frequency shift factors. Figure 6 shows the master curves of PS−host random copolymers with different ^{i}BuPOSS content, wherein data extend over ca. 7 decades of reduced frequency.

Within the temperature range, time−temperature superposition was found to be satisfactory and applicable as expected for single-phase, amorphous polymers far from any thermally stimulated morphological transformation. All of the polymers exhibit a rubbery plateau, terminal zone, and the rubber−liquid transition regimes of viscoelastic behavior. This confirms that all of the samples form entangled melts, as anticipated based on the molecular weight values (Table 1).

The time−temperature superposition shift factor, $a_T(T)$, can be described by the WLF equation,[35] which is derived on the basis of temperature-dependent free volume:

$$\log a_T = \frac{-C_1^g(T - T_g)}{C_2^g + (T - T_g)} \tag{4}$$

Here, $C_1^g = B/2.303f_g$ and $C_2^g = f_g/\alpha_f$, where f_g is fractional free volume at T_g, α_f is the temperature coefficient of fractional free volume, and B is a constant, generally assumed to be unity. If the reference temperature, T_r, is different from glass-transition temperature, the WLF equation will be rewritten as:

$$\log a_T = \frac{-C_1^r(T - T_r)}{C_2^r + (T - T_r)} \tag{5}$$

where $C_1^r = B/2.303f_r$, $C_2^r = f_r/\alpha_f$, and f_r is the fractional free volume at the reference temperature T_r.

Inspection of eq 5 reveals that plots of $1/\log(a_T)$ vs $1/(T-T_r)$ should be linear (if the expression holds) and that the parameters may be determined from the plots' slopes and intercepts. For all random copolymers examined, such plots (Figure 7) indeed feature a linear relationship, indicating validity of eq 5. From the slopes and intercepts, we have determined C_1^r, C_2^r, and f_r for each copolymer, whose values at the glass-transition temperature could be calculated using the following equations.[35]

$$C_1^g = \frac{C_1^r C_2^r}{C_2^r + T_g - T_r} \tag{6}$$

$$C_2^g = C_2^r + T_g - T_r \tag{7}$$

$$f_g = \frac{B(C_2^r + T_g - T_r)}{2.303C_1^r C_2^r} \tag{8}$$

The calculated values of free volume parameters ^{i}BuPOSS−PS random copolymer are tabulated in Table 2. There is not a clear trend in the value of the fractional free volume, f_r, as a function of ^{i}BuPOSS loading at the reference temperature, 120 °C, which is not surprising given the variation in T_g relative to the arbitrary T_r. However, it is very interesting to find that the fractional free volume at T_g (f_g) monotonically decreases with decreasing ^{i}BuPOSS content, where f_g of PS is almost equal to the numerical value reported elsewhere.[36] This result implies that ^{i}BuPOSS molecules can create remarkable void volume in the glass and melts, which leads to associated increases of the

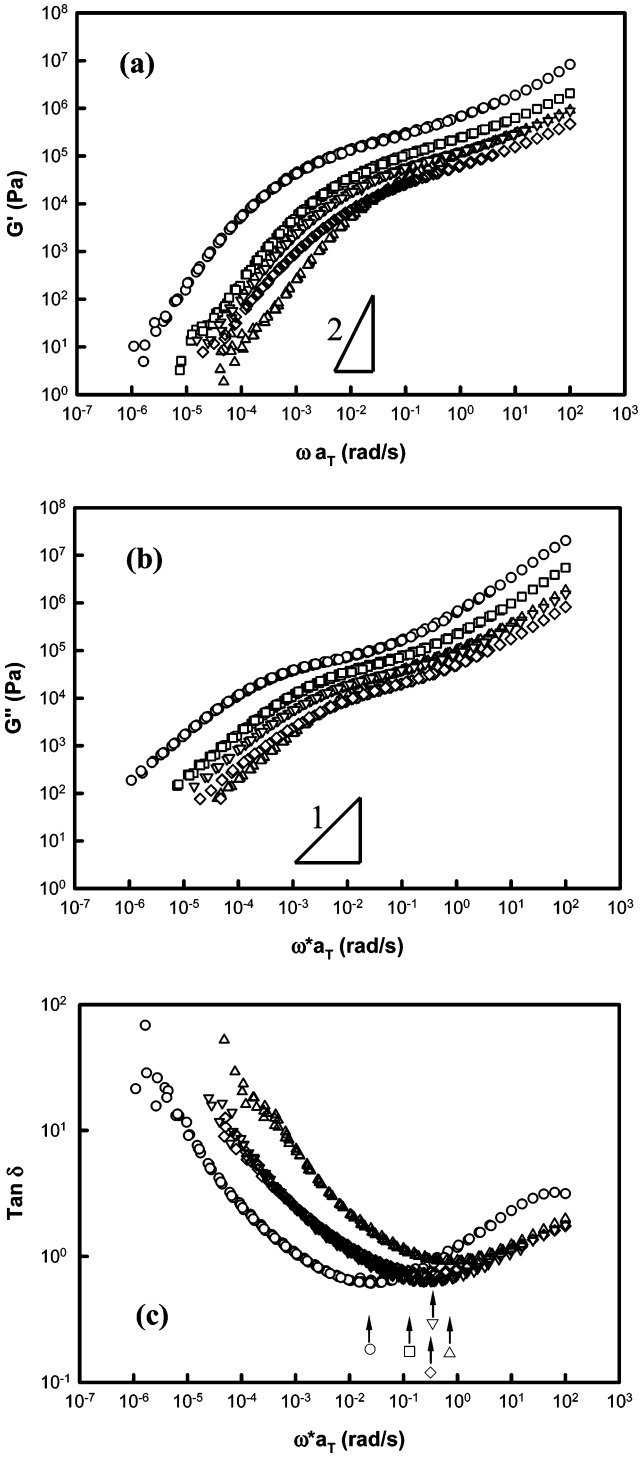

Figure 6. Master curve of as-cast films of ^{i}BuPOSS−PS copolymers with varying weight percentage of ^{i}BuPOSS: (○) 0, (□) 6, (△) 15, (▽) 30, and (◇) 50 wt % ^{i}BuPOSS with $T_r = 120$ °C: (a) G', (b) G'', and (c) tan δ. The arrows in (c) indicate the minimum values of tan δ for each sample.

segmental mobility. The decrease of glass-transition temperature with increasing ^{i}BuPOSS loading observed can be attributed to the additional free volume generated by the tethered POSS molecules.

Meanwhile, the thermal expansivity (α_f) of the fractional free volume also *decreases* with increasing ^{i}BuPOSS loading (Table 2), and at the higher wt % of ^{i}BuPOSS, it seems to level off. In other words, the temperature dependence of fractional free volume is lower for increasing ^{i}BuPOSS content. According to WLF theory (shown in Figure 7 to apply), the fractional free

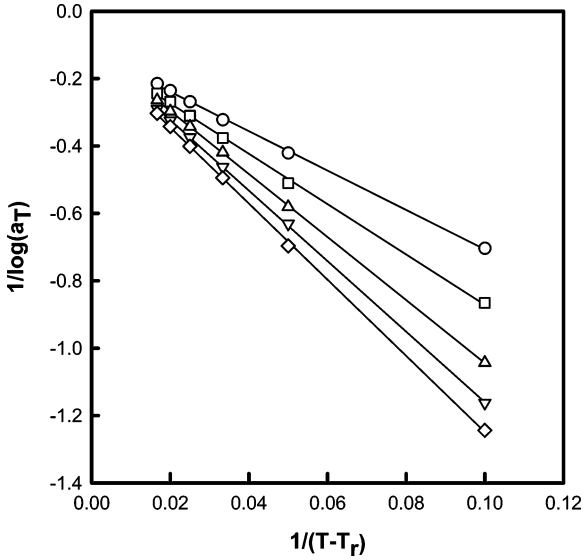

Figure 7. WLF function plot of shift factor for as-cast films of ^{i}BuPOSS−PS copolymers with varying weight percentage of ^{i}BuPOSS: (○) 0, (□) 6, (△) 15, (▽) 30, and (◇) 50 wt % POSS. The reference temperature is 120 °C.

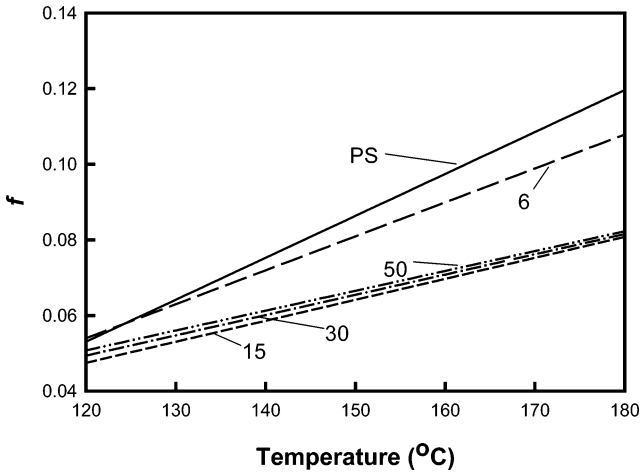

Figure 8. Temperature dependence of fractional free volume (f) as-cast films of ^{i}BuPOSS−PS copolymers with varying weight percentage of ^{i}BuPOSS : (—) 0, (− − −) 6, (−•−•−•) 15, (−••−••−••) 30, and (•••) 50 wt % POSS.

Table 2. Summary of Viscoelastic Characteristics of Polystyrene−POSS Copolymers with Isobutyl R-group at Reference Temperature 120 °C

compound	C_1^r	C_2^r (K)	f_r/B	f_g/B	a_f (K^{-1})
0 wt % ^{i}BuPOSS	8.18	47.85	0.0531	0.0283	11.09×10^{-4}
6 wt % ^{i}BuPOSS	8.05	60.10	0.0540	0.0298	8.98×10^{-4}
15 wt % ^{i}BuPOSS	9.15	85.55	0.0475	0.0319	5.55×10^{-4}
30 wt % ^{i}BuPOSS	8.79	92.04	0.0494	0.0339	5.36×10^{-4}
50 wt % ^{i}BuPOSS	8.55	96.63	0.0508	0.0345	5.25×10^{-4}

volume f can be written approximately as $f = f_g + \alpha_f(T - T_g)$ for $T \geq T_g$. Following this relation and using measured values for all of the parameters, Figure 8 reveals the temperature dependence of free volume fraction for the regime rheologically characterized ($120 < T < 180$ °C) for the ^{i}BuPOSS−PS random copolymers. The PS homopolymer, despite having the lowest fractional free volume at T_g (Table 2), shows the largest value at higher temperature due to its largest α_f value. In contrast, for large ^{i}BuPOSS-content copolymers, the change of fractional free volume with temperature is much smaller. In this sense, the incorporated POSS moieties are somewhat athermal as is the case of inorganic fillers.

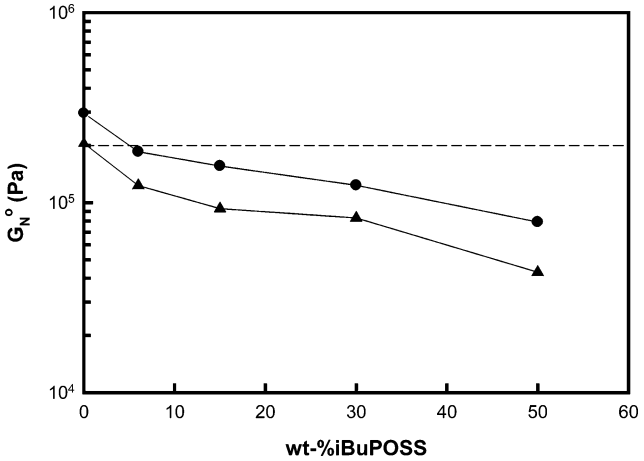

Figure 9. Rubbery plateau modulus (G_N^o) as a function of ^{i}BuPOSS weight fraction: (●) evaluated using eq 9 and (▲) determined from G' at minimum tan δ. The dashed reference line is the plateau modulus of PS reported in ref 36.

3.4.2. Rubbery Plateau. Inspection of Figure 6 reveals not only thermorheological simplicity for all of the copolymers but also a strong dependence of the plateau modulus on level of ^{i}BuPOSS incorporation. In characterizing the rubbery plateau regime, the preferred method to estimate the plateau modulus is to integrate the area under the terminal loss peak[37] in the $G''(\omega)$ spectra. However, due to molecular weight polydispersity (Table 1), our data do not show a peak in loss modulus. Alternately, there are several semiempirical ways to estimate the value of the rubbery plateau, G_N^o. Wu[37] derived eq 9 as an expression relating the crossover modulus, G_c, $[G_c(\omega) = G'(\omega) = G''(\omega)]$ and plateau modulus, G_N^o:

$$\log (G_N^o/G_c) = 0.380 + \frac{2.63(\log p)}{1 + 2.45(\log p)} \qquad (9)$$

where p, the polydispersity index, should be smaller than 3 for the expression to be valid. This equation has been confirmed both theoretically[37,38] and experimentally for many homogeneous polymer melts. A disadvantage, however, is reliance on arguably inaccurate p data. Finally, the method ultimately adopted for plateau modulus measurement utilizes the "tan δ minimum criterion", wherein G_N^o is set equal to the storage modulus G' at the frequency where tan δ is at its minimum in the frequency spectrum:[38,39] $G_N^o = |G'|_{\tan\,\delta\to\min}$. Indeed, Figure 6c revealed that a minimum in tan δ was well-determined for all samples. Figure 9 shows the plateau modulus obtained from these two semiempirical methods in the random copolymer with ^{i}BuPOSS. For both cases, the plateau modulus monotonically decreases with ^{i}BuPOSS content. Moreover the values of G_N^o calculated from the crossover modulus method are slightly higher than those obtained from minimum tan δ. The G_N^o ($\approx 2.0 \times 10^5$ Pa) of PS determined by G' at minimum tan δ is much closer to the value of plateau modulus obtained by integrating the area under the terminal loss peak of monodispersed entangled PS.[36] Henceforth we adopt the "tan δ minimum criterion" as our preferred method.

The relationship between the characteristic value of G_N^o and molecular weight between entanglements, M_e, is:[17,35,40]

$$M_e = \frac{4}{5}\frac{\rho RT}{G_N^o} \qquad (10)$$

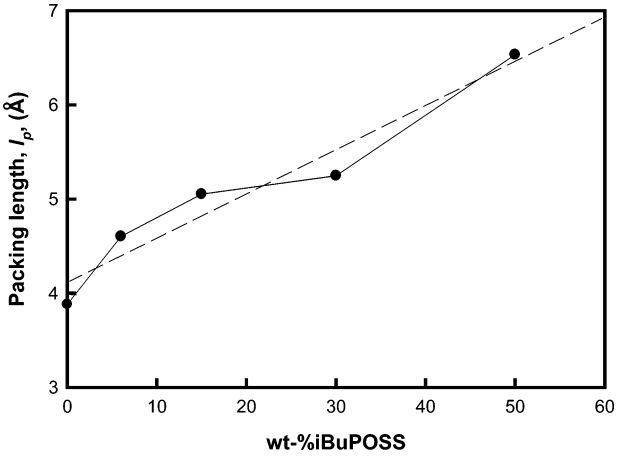

Figure 10. Plot of packing length (l_p) of as-cast films of ^{i}BuPOSS−PS copolymers with varying weight percentage of ^{i}BuPOSS as a function of ^{i}BuPOSS weight fraction. The packing length is calculated using eq 13.

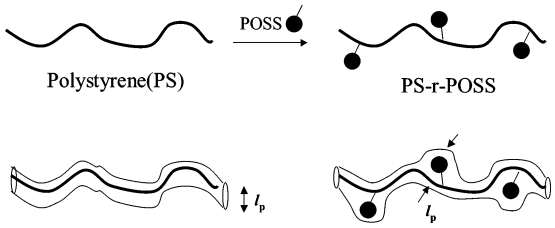

Figure 11. Schematically drawing the effect of the pendent POSS group on the PS chain topology and the resultant tube dimension.

where R is the universal gas constant ($= 8.314$ J·mol^{-1}·K^{-1}), ρ is density, and T is the absolute temperature. The density of PS is 1.05 g/cm^3 at room temperature. Barry[41] and Larsson[42,43] reported crystal densities of POSS-related molecules with different R-groups from CH_3- (1.51 g/cm^3) to n-C_4H_9- (1.14 g/cm^3) to 1-naphthyl− (1.24 g/cm^3). Further, the density of ^{i}BuPOSS has been estimated[15] to be 1.15 g/cm^3. All of these densities are higher than PS at room temperature. Qualitatively, it is reasonable that the density values of random copolymers with different R-group are higher than pure PS, although values of density for ^{i}BuPOSS random copolymers have not been reported. Regardless, melt densities are not expected to change more than several percent between samples, while in contrast, G_N^o values were observed to change nearly an order of magnitude. The temperature-dependent density (ρ, g/cm^3) of pure polystyrene for 100 °C < T < 220 °C can be expressed as follows (T in °C):[44]

$$\rho = 1.0865 - 6.19 \times 10^{-4} T + 0.136 \times 10^{-6} T^2 \qquad (11)$$

Assuming such temperature-dependent density values, even for our copolymers, the entanglement molecular weight and the number of entanglements per chain of our ^{i}BuPOSS−PS copolymers calculated from eq 10 are detailed in Table 3. One can observe that the entanglement molecular weight clearly increases with ^{i}BuPOSS loading. In effect, ^{i}BuPOSS incorporation along the PS chain dilutes the entanglement density. Meanwhile, the entanglements per chain of our copolymers vary in a range from ∼7 to ∼13, which further confirms that all of the samples effectively entangled, as anticipated based on the molecular weight. The terminal slopes also listed in Table 3 will be discussed later.

From the viewpoint of chemical structure, POSS groups grafted on the PS chain play the same role of branches and

Table 3. Rheological Properties of Polystyrene−POSS Copolymers with Isobutyl R-group

compound	G_N^0 (kPa)	M_e (kg/mol)	$Z = M_w/M_e$	$(dG'/da_T\omega)_{\omega\to 0}$	$(dG''/da_T\omega)_{\omega\to 0}$
0 wt % ^{i}BuPOSS	205	12.9	12.5	1.65	0.99
6 wt % ^{i}BuPOSS	123	21.5	8.6	1.44	0.98
15 wt % ^{i}BuPOSS	93	28.5	6.8	1.35	0.97
30 wt % ^{i}BuPOSS	83	31.9	9.4	1.33	0.96
50 wt % ^{i}BuPOSS	42	61.6	6.8	1.27	0.93

essentially change the topology of the PS chain. There have been very extensive studies on the effects of microscopic topology on the rheological behavior in the entangled polyolefin liquids.[45−48] However, careful studies on randomly branched polystyrene have received less attention.[49−51] These studies mainly focused on the effect of the long chain branches (LCBs) on the linear and nonlinear rheological properties. How spherical cagelike branches, such as POSS molecules, affect the rheological behavior has not been studied.

Fetters et al.[18] developed the relationship between the entanglement density of polymer species and their molecular dimensions in the melt state, resulting in the expression

$$M_e = 218 \times 10^{-6}\, \rho l_p^{\,3} \tag{12}$$

where l_p (Å) is the packing length defined as the occupied volume of a chain divided by the mean-square end-to-end distance, M_e (kg/mol) is the entanglement molecular weight, ρ (kg/mol) is the density, and the units of the prefactor, 218×10^{-6}, is $m^3 \cdot mol^{-1} \cdot Å^{-3}$. Roughly, this length may be interpreted as the effective chain profile or width. Combining eqs 10 and 12 allows a density-independent determination of l_p from G_N^o

$$l_p = \left(3.67 \times 10^3 \frac{RT}{G_N^o}\right)^{1/3} \tag{13}$$

where R ($J \cdot mol^{-1} \cdot K^{-1}$) is the universal gas constant, T (K) is absolute temperature, G_N^o (Pa) is the rubbery plateau modulus, and prefactor units, 3.67×10^3, are $Å^3 \cdot m^{-3} \cdot mol^{-1}$. Thus, smaller plateau moduli imply larger l_p, or chain profiles, as well as larger tube diameters d_t ($d_t = 19 l_p$).[18]

By using eq 13 and the plateau modulus data of Figure 9, we computed values of l_p for ^{i}BuPOSS−PS random copolymers (Figure 10). We find that the packing length monotonically increases from a value of 3.88 Å for PS homopolymer (reported elsewhere as 3.92 Å)[18] to a value at 6.63 Å for 50 wt % (10.95 mol %; ≈ 1 in 10 repeat units bearing a POSS branch). This is a very large packing length increase (71%). A similar increase (73%) is observed in polymethacrylates when the pendent methyl group of PMMA is uniformly (every repeat unit) substituted by an octyl group.[18] Thus, substituting one ^{i}BuPOSS on every tenth repeating unit of a PS chain is topologically equivalent to substituting every repeat unit of a PMA chain with an *n*-octyl chain. Interestingly enough, ten *n*-octyl chains feature a molecular weight of 1130 g/mol, comparable to (but larger than) the molecular weight of each pendent POSS moiety, 816 g/mol. Certainly, the estimated values of packing length of ^{i}BuPOSS−PS copolymers should be confirmed further by other observations, such as small-angle neutron scattering (SANS), and employing finer synthetic methods to prepare the narrow polydispersity samples.

From this topological viewpoint, we can explain the observed dependence of plateau modulus on ^{i}BuPOSS content. A schematic drawing to describe the effect of pendent ^{i}BuPOSS groups on the dimension of the reptation tube, l_p or d_t, is shown in Figure 11. Undoubtedly, the pendent ^{i}BuPOSS has a great influence on the PS chain topology. Presuming that the dynamics of the present random copolymers follow the tube model, the resultant average tube diameter will increase due to the presence of the pendent ^{i}BuPOSS molecules and consequently lower the entanglement density. We envision that the average tube diameter of the constituted PS chains increases with the increasing POSS content. Consequently, the plateau modulus monotonically decreases with increasing POSS content due to the variation of microscopic topology of PS chain.

Possible intermolecular interactions have been ignored in the discussions above. If strong intermolecular interactions were to exist, then the plateau modulus would be enhanced and there would be two dominant mechanical relaxations above the glass-transition temperature (T_g): one from disentanglement and the other from disassociation of specific intermolecular interaction. These mechanisms together are encapsulated in a "sticky reptation" model developed by Liebler et al.[10] conceived for hydrogen-bonded elastomers. Although the interaction due to the individual R-groups is weak, each POSS cage contains seven of them, resulting in multiple interactions that may magnify the total interaction of each POSS cage. Romo-Uribe et al.[9] observed the rheological behavior in the unentangled random copolymers styryl CpPOSS or styryl CyPOSS and 4-methylstyrene. There, when POSS loading was increased beyond a critical value, a terminal zone region could not be reached at any high temperature or low frequency, and a secondary rubbery plateau appeared. In particular, they observed the critical value for this transformation that depended on R-group: CpPOSS was around 60 wt %, while CyPOSS was at 40 wt %.

In our case, the ^{i}BuPOSS molecules pendent to the PS chain are dispersed at the molecular level, and no obvious aggregation is observed. The primary attractive force of interaction is between ^{i}BuPOSS and PS segments. Nevertheless, we observed only a single mechanical relaxation above T_g, this being due to chain diffusion relaxing stress. Thus we can propose that the interaction between ^{i}BuPOSS and PS matrix is weak and incapable of yielding a secondary rubbery plateau. In our random copolymers from styrene− and styryl−^{i}BuPOSS, the effect of ^{i}BuPOSS on the microscopic chain topology is the dominant effect on the plateau modulus. Meanwhile, it can also be expected that the interaction between the POSS and PS matrixes is tunable by varying the R-group. Indeed, the R-group dependence of rheological behavior will be discussed in a following paper.

Within the rubbery plateau regime, polymers with linear chain branches normally follow two kinds of relaxation mechanisms below the dynamic glass transition:[52,53] the branches relax with the rapid Rouse motion (or rapid reptation) at higher frequencies, with the effective tube diameter increasing continuously until the branch arms are completely retracted. Then the primary backbone follows reptation-like relaxation in the widened tubes at lower frequencies. Thus, there are two separated relaxation scales, a shorter one for branches and a longer one for the backbone. However, all of the master curves shown in Figure 6 do not feature such a relaxation at the higher frequencies, instead featuring only one characteristic relaxation. We attribute this finding to the fact that POSS branches are different from the common polymeric coil branches. In particular, they feature

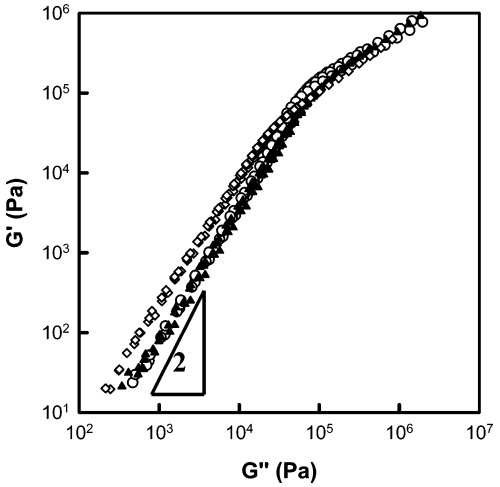

Figure 12. Double logarithm plot of G' vs G'' for as-cast films of ^{i}BuPOSS−PS copolymers with varying weight percentage of ^{i}BuPOSS: (○) 0, (▲) 15, and (◇) 50 wt % ^{i}BuPOSS.

a compact, nanoscale structure incapable of entangling and thus experiencing associated mechanical relaxation.

3.4.3. Behavior in Terminal Zone. Within the terminal zone, polymer melts should be fully relaxed and follow the characteristic power laws for frequency dependence of the shear storage and loss moduli: $G' \sim \omega^2$ and $G'' \sim \omega$.[1] The slopes of terminal zones were estimated for random copolymers with variation in ^{i}BuPOSS content and reported in Table 3. The terminal zone frequency dependence of the storage modulus decreases with the increased ^{i}BuPOSS from $\omega^{1.65}$ for pure PS to $\omega^{1.27}$ for 50 wt % ^{i}BuPOSS. Meanwhile, there also appears to be a slight decrease in the power-law exponent for G'' with ^{i}BuPOSS loading, from $\omega^{0.99}$ for pure PS to $\omega^{0.93}$ for 50 wt % ^{i}BuPOSS. According to Doi−Edwards reptation theory,[17] the relationship between G' and G'' for the linear flexible polymer can be expressed as

$$\log G' = 2 \log G'' - \log(\rho RT/M_e) + \log(\pi^2/8) \quad (14)$$

where ρ is the density, R is universal gas constant, and T is the absolute temperature. We note that such a plot is independent of molecular weight. For the ideal polymeric liquid, the slope of log G' versus log G'' is 2 in the terminal zone, while the intercept can directly yield G_N^o. Figure 12 shows the logarithmic plot of G' and G'' (termed the Han plot[54]) with different ^{i}BuPOSS loading.

Like the frequency dependence of G', the slope of G' versus G'' also has an ^{i}BuPOSS content dependence. In particular, the slope decreases with increasing ^{i}BuPOSS loading. Compared with the tendency of molecular weight polydispersity with ^{i}BuPOSS content, we cannot attribute this deviation from the classical terminal behavior only to the effect of molecular weight polydispersity. Instead, intermolecular interactions may play a role. Morphological characterization showed us that the pendent ^{i}BuPOSS groups are dispersed at nearly a molecular level. We argue then that the deviation from the classical terminal behavior may be ascribed to the existence of finite interactions between ^{i}BuPOSS and PS segments. Although the primary attraction force of interaction between POSS and PS-matrix is weak and, therefore, less important in the rubbery plateau frequency regime (where stresses are higher), this interaction could reasonably have influence on the terminal zone behavior as reflected in the Han-plot slope.

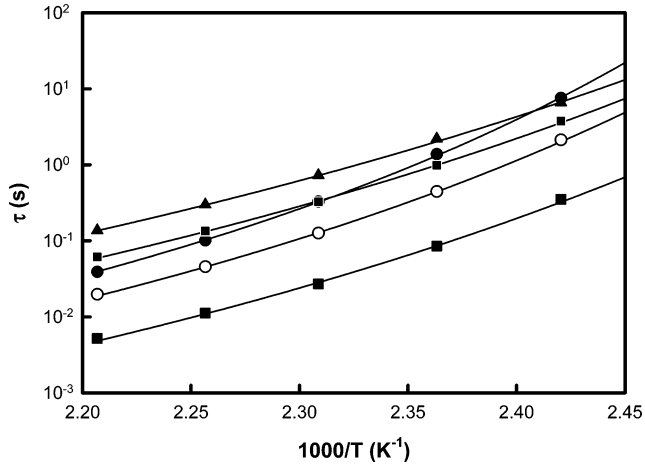

Figure 13. Temperature dependence of terminal zone relaxation time (τ) for as-cast films of ^{i}BuPOSS−PS copolymers as a function of POSS weight fraction: (●) 0, (○) 6, (■) 15, (□) 30, and (▲) 50 wt % ^{i}BuPOSS. The solid lines represent the best-fit VFTH curves for the copolymers and PS homopolymer.

We now consider the terminal relaxation time as influenced by ^{i}BuPOSS incorporation. Due to significant variation in molecular weight of the copolymer series (Table 1), we focus on the temperature dependence of the terminal relaxation time, rather than the absolute values. The terminal zone can be characterized by several parameters, including the terminal relaxation time, τ, the zero shear viscosity η_0, and steady-state shear compliance J_e^o, defined in the usual manner. Accordingly, the relaxation time values for each copolymer could be determined from zero-frequency limits of storage and loss modulus spectra obtained at different temperatures.

The temperature dependences of the ^{i}BuPOSS−PS copolymer terminal relaxation times were well described by the Vogel−Fulcher−Tamman−Hesse (VFTH) equation:[55−57]

$$\tau = A \exp\left(\frac{B}{T - T_0}\right) \quad (15)$$

where T_0 is the "ideal glass-transition temperature" (or "Vogel temperature"), and B is termed an "apparent activation energy," physically representing an Arrhenius-like temperature activation energy (although with units of temperature). Figure 13 shows the temperature dependence of terminal relaxation times of the polystyrene− and styryl−^{i}BuPOSS random copolymers, together with the best-fit VFTH curves. The values of T_0 and B, extracted from the best-fit VFTH equation curves, are reported as a function of ^{i}BuPOSS content in Figure 14. We observed that the "apparent activation energy", B, increases by ca. 50% and T_0 decreases by ca. 40 °C when POSS loading is increased from 0 to 50 wt %. (Note by inspection of eq 15 that *increasing* B corresponds to *decreasing* temperature sensitivity.) Thus, similar to our observations of decreasing α_f with increasing POSS loading (Table 2), we observed a lowering of the temperature sensitivity for the terminal relaxation time with ^{i}BuPOSS copolymerization, as manifested in the VFTH B "activation energy" parameter.

There are several theoretical models to explain the effects of branches on the temperature dependence of terminal relaxation time. According to the coupling model,[58−60] the dynamics of polymer chains can be described by the coupling parameter n ($0 < n < 1$), where the value of n is closely related to the topological constraints of the entangled system. The surrounding environment experienced by a single macromolecular chain is the key factor of this parameter. In particular, the parameter

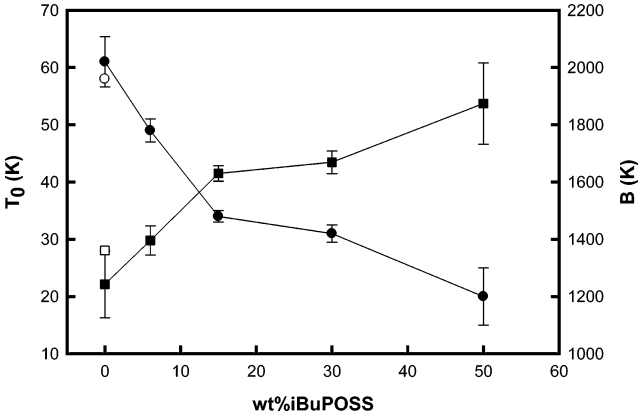

Figure 14. Plot of Vogel temperature (T_0, ●) and apparent activation energy (B, ■) of ^{i}BuPOSS−PS copolymers as a function of ^{i}BuPOSS content, which are extracted from the best-ft curves shown in Figure 14. The symbols of open circle (○) and open square (□) are the values of T_0 and B for PS from ref 51.

values for linear and branched polymers are related by their corresponding activation energies:

$$\frac{E_{\text{branch}}}{E_{\text{linear}}} = \frac{1 - n_{\text{linear}}}{1 - n_{\text{branch}}} \tag{16}$$

The coupling model predicts that the temperature dependence of branched polymers will always be weaker (larger E) than that of the corresponding linear polymers, as $n_{\text{branch}} > n_{\text{linear}}$. More specifically, branched polymers are expected to have stronger "coupling" that acts to increase n, resulting in broadening of the relaxation function and increasing activation energy of the rheological properties. Usually, this model is valid for branched polymers for which the molecular weight of branches exceeds the entanglement molecular weight, M_e.[58−60] However, only a few studies have been reported for branched polystyrene.[49−51] Ferri et al.[51] prepared randomly branched polystyrene by copolymerization of styrene (St) and divinylbenzene (DVB) and studied the melt rheology of linear and randomly branched polystyrene (LPS ad RBPS), where the RBPS featured entangled branches ($M_{\text{br}}/M_e > 4$). They found that, while the shift factors (a_T) of LPS were similar to those of RBPS, the activation energy slightly increased with degree of branching. Our results are qualitatively consistent with these RBPS[51] data despite architectural dissimilarity.

Semiquantitative comparison of our observations with atomistic molecular dynamics simulations is also possible. In particular, simulations of POSS−polynorbornene random copolymers due to Bharadwaj, Berry, and Farmer[5] indicated a weaker temperature dependence of elastic moduli for CyPOSS− and CpPOSS−polynorbornene copolymers than for the reference PN homopolymer, consistent with our present observations of increasing VFTH apparent activation energy. There, it was reasoned that POSS units act as an "anchor" against molecular motion. While it would seem that such anchoring effect would be most important at short time scales, not within the terminal zone, it is reasonable that the nature of polymer reptation with periodic "anchors" requires attention at the level of polymer chain diffusion calculations. To finally elucidate this aspect, finer synthetic methods to prepare the narrow dispersed random copolymers from styrene and styryl ^{i}BuPOSS are needed.

4. Conclusions

We investigated the thermal and linear rheological behavior of random copolymers from styrene- and styryl-based ^{i}BuPOSS. The molecularly homogeneous copolymers featured decreasing T_g with increasing ^{i}BuPOSS incorporation, a finding attributed to increased free volume. The dynamic moduli were measured within the linear viscoelastic regime over a range of temperatures from 120 to 180 °C. Rheological characterization showed that time−temperature superposition (TTS) works well over a range of ^{i}BuPOSS content up to 50 wt %. The well-fitted WLF equation revealed that the fractional free volume at T_g, f_g, increases with the ^{i}BuPOSS loading; however, the corresponding temperature coefficient of free volume was seen to decrease with increasing ^{i}BuPOSS content. We propose that the ^{i}BuPOSS groups play a plasticizer-like role in determining the glass-transition temperature, increasing the glassy free volume fraction to enhance the PS segmental mobility.

Compared with the linear-branched polymers, there is no branch (arm) retraction mechanism at the short times observed in our PS branched by ^{i}BuPOSS. The rubbery plateau modulus, defined as the shear storage modulus at the condition of minimum loss tangent, decreases with increasing ^{i}BuPOSS incorporation, which we parametrized as an increasing tube diameter and thus packing length due to the presence of the ^{i}BuPOSS group along the PS chain, making the polymer chain "bulky", diluting the entanglement density. Within the terminal zone, the shear storage modulus $G'(\omega)$ featured deviation from an ideal liquid with increasing POSS content; however, no secondary rubbery plateau was observed. This indicated that the interaction between ^{i}BuPOSS groups within PS segments is not sufficient to yield "sticky reptation"-like behavior. The terminal relaxation times were found to have weaker temperature dependence for random copolymer with ^{i}BuPOSS than for the pure linear PS homopolymer, the apparent activation energy increasing with increasing ^{i}BuPOSS loading. Like linear polymeric coil branches, the ^{i}BuPOSS cage plays a negative effect on the temperature dependence of terminal relaxation time. This phenomenon seems consistent with the coupling model and with large-scale molecular dynamics simulations.

Acknowledgment. This research was sponsored by Air Force Research Lab, Propulsion Directorate, Edwards AFB.

Supporting Information Available: The linear viscoelastic data shown in Figure 6 are plotted in the form of a van Grup−Palmen plot. This material is available free of charge via the Internet at http://pubs.acs.org.

References and Notes

(1) Li, G.; Wang, L.; Ni, H.; Pittman, C. U., Jr. *J. Inorg. Organomet. Polym.* **2002**, *11*, 123−154.
(2) Haddad, T. S.; Lichtenhan, J. D. *Macromolecules* **1996**, *29*, 7302−7304.
(3) Mather, P. T.; Jeon, H. G.; Romo-Uribe, A.; Haddad, T. S.; Lichtenhan, J. D. *Macromolecules* **1999**, *32*, 1194−1203.
(4) Lichtenhan, J. D.; Otonari, Y. A.; Carr, M. J. *Macromolecules* **1995**, *28*, 8435−8437.
(5) Bharadwaj, R. K.; Berry, R. J.; Farmer, B. L. *Polymer* **2000**, *41*, 7209−7221.
(6) Lee, A.; Lichtenhan, J. D. *Macromolecules* **1998**, *31*, 4970−4974.
(7) Li, G. Z.; Wang, L.; Toghiani, H.; Daulton, T. L.; Koyama, K.; Pittman, C. U., Jr. *Macromolecules* **2001**, *34*, 8686−8693.
(8) Li, G. Z.; Wang, L.; Toghiani, H.; Daulton, T. L.; Pittman, C. U., Jr. *Polymer* **2002**, *43*, 4167−4176.
(9) Romo-Uribe, A.; Mather, P. T.; Haddad, T. S.; Lichtenhan, J. D. *J. Polym. Sci., Part B: Polym. Phys.* **1998**, *36*, 1857−1872.
(10) Leibler, L.; Rubinstein, M.; Colby, R. H. *Macromolecules* **1991**, *24*, 4701−4707.
(11) Delucca Freitas, L. L.; Stadler, R. *Macromolecules* **1987**, *20*, 2478−2485.
(12) Stadler, R.; Delucca Freitas, L. L. *Colloid Polym. Sci.* **1986**, *264*, 773−778.

(13) Loveless, D. M.; Jeon, S. L.; Craig, S. L. *Macromolecules* **2005**, *38*, 10171−10177.
(14) Vermonden, T.; van Steenbergen, M. J.; Besseling, N. A. M.; Marcelis, A. T. M.; Hennink, W. E.; Sudholert, E. J. R.; Cohen Stuart, M. A. *J. Am. Chem. Soc.* **2004**, *126*, 15802−15808.
(15) Kopesky, E. T.; Haddad, T. S.; Cohen, R. E.; McKinley, G. H. *Macromolecules* **2004**, *37*, 8992−9004.
(16) Kopesky, E. T.; Haddad, T. S.; McKinley, G. H.; Cohen, R. E. *Polymer* **2005**, *46*, 4743−4752.
(17) Doi, M.; Edwards, S. F. *The Theory of Polymer Dynamics*; Clarendon: Oxford, 1986.
(18) Fetters, L. I.; Lohse, D. I.; Graessley, W. W. *J. Polym. Sci., Part B: Polym. Phys.* **1999**, *37*, 1023−1033.
(19) Everaers, R.; Sukumaran, S. K.; Grest, G. S.; Svaneborg, C.; Sivasubramanian, A.; Kremer, K. *Science* **2004**, *303*, 823−827.
(20) Moore, B. M.; Haddad, T. S.; Gonzalez, R. I.; Schlaefer, C. *Polym. Prepr. (Am. Chem. Soc., Div. Polym. Chem.)* **2004**, *45*, 692−693.
(21) Kim, G.-M.; Qin, H.; Fang, X.; Sun, F. C.; Mather, P. T. *J. Polym. Sci., Part B: Polym. Phys.* **2003**.
(22) Atkins, E. D. T.; Isaac, D. H.; Keller, A.; Miyasaka, K. *J. Polym. Sci., Polym. Phys. Ed.* **1977**, *15*, 211−226.
(23) Mitchell, G. R.; Windle, A. H. *Polymer* **1984**, *25*, 906−920.
(24) Waddon, A. J.; Coughlin, E. B. *Chem. Mater.* **2003**, *15*, 4555−4561.
(25) Fu, B. X.; Zhang, W.; Hsiao, B. S.; Rafailovich, M.; Sokolov, J.; Johansson, G.; Sauer, B. B.; Phillips, S.; Balnski, R. *High Perform. Polym.* **2000**, *12*, 565−571.
(26) Leu, C.-M.; Reddy, G. M.; Wei, K.-H.; Shu, C.-F. *Chem. Mater.* **2003**, *15*, 2261−2265.
(27) Zheng, L.; Hong, S.; Cardoen, G.; Burgaz, E.; Gido, S. P.; Coughlin, E. B. *Macromolecules* **2004**, *37*, 8606-8611.
(28) Chen, W. Y.; Ho, K. S.; Hsieh, T. H.; Chang, F. C.; Wang, Y. Z. *Macromol. Rapid Commun.* **2006**, *27*, 452−457.
(29) Zhang, W.; Fu, B. X.; Seo, Y.; Schrag, E.; Hsiao, B.; Mather, P.; Yang, N.-L.; Xu, D.; Ade, H.; Rafailovich, M.; Sokolov, J. *Macromolecules* **2002**, *35*, 8029−8038.
(30) Rogers, S.; Mandelkern, L. *J. Phys. Chem.* **1957**, *61*, 985−991.
(31) Haddad, T. S.; Choe, E.; Lichtenhan, J. D. *Mater. Res. Soc. Symp. Proc.* **1996**, *435*, 25−32.
(32) Lichtenhan, J. D.; Vu, N. Q.; Carter, J. A.; Gillman, J. W.; Feher, F. J. *Macromolecules* **1993**, *26*, 2141−2142.
(33) Xu, H.; Kuo, S.-W.; Lee, J.-S.; Chang, F.-C. *Polymer* **2002**, *43*, 5117−5124.
(34) Xu, H.; Kuo, S. W.; Lee, J. S.; Chang, F. C. *Macromolecules* **2002**, *35*, 8788−8793.
(35) Ferry, J. D. *Viscoelastic Properties of Polymers*, 3rd ed.; John Wiley & Sons, New York, 1980.
(36) Onogi, S.; Masuda, T.; Kitagawa, K. *Macromolecules* **1970**, *3*, 109−116.
(37) Wu, S. *J. Polym. Sci., Part B: Polym. Phys.* **1989**, *27*, 723−741.
(38) Wu, S. *J. Polym. Sci., Part B: Polym. Phys.* **1987**, *25*, 2511−2529.
(39) Wu, S. *J. Polym. Sci., Part B: Polym. Phys.* **1987**, *25*, 557−566.
(40) Larson, R. G.; Sridhar, T.; Leal, L. G.; McKinley, G. H.; Likhtman, A. E.; McLeish, T. C. B. *J. Rheol.* **2003**, *47*, 809−818.
(41) Barry, A. J.; Daudt, W. H.; Domicone, J. J.; Gilkey, J. W. *J. Am. Chem. Soc.* **1955**, *77*, 4248−4252.
(42) Larsson, K. *Ark. Kemi* **1960**, *16*, 203−208.
(43) Larsson, K. *Ark. Kemi* **1960**, *16*, 209−214.
(44) Höcker, H.; Blake, G. J.; Flory, P. J. *Trans. Faraday Soc.* **1971**, *67*, 2251−2257.
(45) McLeish, T. *NATO ASI Ser., Ser. E* **1997**, *339*, 87−113.
(46) McLeish, T. *Math. Chem.* **1999**, *5*, 265−315.
(47) McLeish, T. C. B. *Adv. Phys.* **2002**, *51*, 1379−1527.
(48) Vlassopoulos, D.; Fytas, G.; Pakula, T.; Roovers, J. *J. Phys.: Condens. Matter* **2001**, *13*, R855−R876.
(49) Rooves, J. *Macromolecules* **1984**, *17*, 7521−7526.
(50) Masuda, T.; Ohta, Y.; Onogi, S. *Macromolecules* **1986**, *19*, 2524−2532.
(51) Ferri, D.; Lomellini, P. *J. Rheol.* **1999**, *43*, 1355−1372.
(52) McLeish, T. C. B.; Allgaier, J.; Bick, D. K.; Bishko, G.; Biswas, P.; Blackwell, R.; Blottière, B.; Clarke, N.; Gibbs, B.; Groves, D. J.; Hakiki, A.; Heenan, R. K.; Johnson, J. M.; Kant, R.; Read, D. J.; Young, R. N. *Macromolecules* **1999**, *32*, 6734-6758.
(53) Daniels, D. R.; McLeish, T. C. B.; Crosby, B. J.; Young, R. N.; Fernyhough, C. M. *Macromolecules* **2001**, *34*, 7025−7033.
(54) Han, C. D.; Kim, J. H. *J. Polym. Sci., Part B: Polym. Phys.* **1987**, *25*, 1741−1764.
(55) Vogel, H. *Phys. Z.* **1921**, *22*, 645−646.
(56) Tamman, G.; Hesse, W. Z. *Z. Anorg. Allg. Chem.* **1926**, *156*, 245−257.
(57) Fulcher, G. S. *J. Am. Ceram. Soc.* **1925**, *8*, 339−355.
(58) Carella, J. M.; Gotro, J. T.; Graessley, W. W. *Macromolecules* **1986**, *19*, 659−667.
(59) Bero, C. A.; Roland, C. M. *Macromolecules* **1996**, *29*, 1562−1568.
(60) Ngai, K. L.; Roland, C. M. *J. Polym. Sci., Part B: Polym. Phys.* **1997**, *35*, 2503−2510.

MA061886F